Small-angle X-ray scattering from sodium hyaluronate in aqueous sodium chloride

Naoya Mizukoshi, Takashi Norisuye

Department of Macromolecular Science, Osaka University, Toyonaka, Osaka 560, Japan

Summary

Four narrow-distribution samples of sodium hyaluronate with weight-average molecular weights M_w of 3.8 x 10^3 to 1.1 x 10^4 in 0.02 and 0.1 M aqueous NaCl at 25ºC have been studied by small-angle X-ray scattering. Data for their z-average radii of gyration $\langle S^2 \rangle_z^{1/2}$ and particle scattering functions $P(\theta)$, together with previous $\langle S^2 \rangle_z$ data from light scattering for high molecular weights, are compared with relevant theories for the wormlike chain with or without excluded volume, using the parameters estimated previously from intrinsic viscosity ($[\eta]$) data. It is shown that for M_w lower than 1.1 x 10^4, $\langle S^2 \rangle_z$, $P(\theta)$, and $[\eta]$ of the polysaccharide in the aqueous salts are all consistently explained by this model without excluded volume.

Introduction

Our understanding of intramolecular excluded-volume effects in linear polyelectrolytes still remains in an unsatisfactory stage. The primary difficulty in the experimental study on those polymers is that without relevant theory, the effects of chain stiffening and volume exclusion on measured properties can hardly be separated.

In previous work (1,2), we estimated the persistence length q (or the stiffness parameter) and the linear mass density M_L for sodium hyaluronate, a charged linear polysaccharide, in aqueous NaCl as a function of salt concentration C_s by analyzing intrinsic viscosity ($[\eta]$) data on the basis of the theory (3,4) for the wormlike chain (5) combined with the quasi-two-parameter (QTP) theory (6) for nonionic chains. Subsequently (7), it was found that when these parameters, together with the excluded-volume strength estimated from $[\eta]$, are used, the QTP theory (6) almost quantitatively explains the measured (light scattering) z-average radii of gyration $\langle S^2 \rangle_z^{1/2}$ for high molecular weight samples at $C_s \geq 0.02$ M. Apparently, this finding on the applicability of the theory to the polyelectrolyte builds on the unperturbed dimensions estimated indirectly from $[\eta]$. Thus, we deemed it necessary to check whether the q and M_L values from $[\eta]$ are indeed consistent with $\langle S^2 \rangle_z$ and the particle scattering function $P(\theta)$ for low molecular weight hyaluronate samples for which intramolecular excluded-volume effects are negligible.

In the present work, such samples were prepared and studied by small-angle X-ray scattering (SAXS) at $C_s = 0.02$ and 0.1 M. The results obtained for $<S^2>_z$ and $P(\theta)$ and their analyses are presented below..

Experimental

Samples

A hyaluronate sample with a purity higher than 99% ([η] in 0.2 M aqueous NaCl at 25ºC = 2560 CM³ g⁻¹), supplied by Shiseido Co., Japan, was degraded to short chains by heating at 110ºC (48 - 60 h) followed by hydrolysis with 1 N aqueous hydrochloric acid at 50ºC (5 - 11 h). After being neutralized with aqueous sodium hydroxide, the resulting samples ([η] in 0.2 M aqueous NaCl = 10 - 60 cm³ g⁻¹) were fractionated extensively by repeating fractional precipitation with 0.5 M aqueous sodium acetate as the solvent and ethanol as the precipitant. From 32 middle fractions thus obtained, four samples designated below as HAM1, HAM2, HAM3, and HAM4 were chosen for the present study. They were converted to the Na salt form and dried as described previously (1).

Sedimentation Equilibrium and Viscometry

Weight-average molecular weights M_w and z-average to weight-average molecular weight ratios M_z/M_w for the four samples were determined by sedimentation equilibrium in a Beckman Model E ultracentrifuge with 0.5 M aqueous NaCl at 25ºC as the solvent (see ref. 1 for the experimental details).

We also made viscosity measurements on the four samples in 0.02 and 0.1 M aqueous NaCl at 25ºC in order to confirm the previous [η] - M_w relations (2) in a low molecular weight region. According to our previous analysis (2), [η] of Na hyaluronate in the aqueous salts is essentially unperturbed by volume effect if M_w is lower than 1.5 x 10⁴.

SAXS

Intensities of X-ray scattered from Na hyaluronate in 0.02 and 0.1 M aqueous NaCl at 25ºC were measured on a SAXS apparatus (8,9) equipped with an imaging plate (IP) detector, using the Kα line (wavelength $\lambda_0 = 0.154$ nm) as the incident X-ray beam and a quartz capillary of 1.5-mm diameter as the scattering cell. The observed two-dimensional scattering profile on an IP was processed by an IP reading system (Rigaku R-AXIS DS), and the scattering intensity at scattering angle θ was obtained by integration of intensities in an angular range from $\theta - \Delta\theta$ to $\theta + \Delta\theta$, with $\Delta\theta$ taken as 0.04º (see ref. 8); note that our apparatus requires no desmearing procedure.

Data for each solution or solvent were accumulated for 20 h, since intensities from hyaluronate solutions were very weak in the range of c (the polymer mass concentration) studied (for example, 0.01 - 0.04 g cm⁻³ for HAM1 and 0.03 - 0.09 g cm⁻³ for HAM4).

Nonetheless, the excess scattering intensities ΔI_θ obtained were not very accurate for k [$\equiv$ $(4\pi/\lambda_0)\sin(\theta/2)$] greater than 0.8 - 0.9 nm^{-1}, and only those for $k \leq 0.9$ nm^{-1} were extrapolated to infinite dilution using the square-root plot of $(c/\Delta I_\theta)^{1/2}$ vs. c. It should be noted that no accurate theoretical $P(\theta)$ of the wormlike chain (to be compared with our experiment) is as yet available for $2qk$ greater than 10, i.e., for $k > 0.83$ nm^{-1} in the case of Na hyaluronate in 0.02 M aqueous NaCl ($q = 6$ nm).

Results

Table I summarizes molecular weight data from sedimentation equilibrium. All our samples have molecular weights lower than the above-mentioned critical value 1.5 x 10^4 below which $[\eta]$ exhibited substantially unperturbed behavior. The M_z/M_w values indicate that these samples are fairly narrow in molecular weight distribution. The second virial coefficients (at $C_s = 0.5$ M) were 3.0 x 10^{-3} - 4.9 x 10^{-3} Mol g^{-2} cm^3 (not shown here).

Figure 1 shows the plots of $P(\theta)^{-1/2}$ vs. k^2 (at low angles) for the four samples in 0.02 M aqueous NaCl. The circles with pip represent the additional data obtained for $\Delta\theta = 0.02°$. The values of $<S^2>_z^{1/2}$ evaluated from the indicated dashed lines (the initial slopes of the plots) are presented in the fourth and fifth columns of Table I. We note that they are free from the effect of chain thickness but may contain an error of about ±5%.

The $[\eta]$ data obtained are given in the last two columns of Table I. We have ascertained that they fall on the theoretical $[\eta]$ versus molecular weight curves fitting the previous data (2, 7) at $C_s = 0.02$ and 0.1 M (not shown here) and thus exhibit the unperturbed wormlike chain behavior; as shown previously (2), the theoretical curves with and without excluded volume overlap with each other for molecular weights below 1.5 x 10^4. The parameters (q, M_L, and the excluded-volume strength B) from (η) at $C_s = 0.02$ and 0.1 M are presented in Table II for convenience of our ensuing analysis of $<S^2>_z$ and $P(\theta)$.

Table I. Results from Sedimentation Equilibrium, SAXS, and Viscosity Measurements on Na Hyaluronate Samples in Aqueous NaCl at 25°C

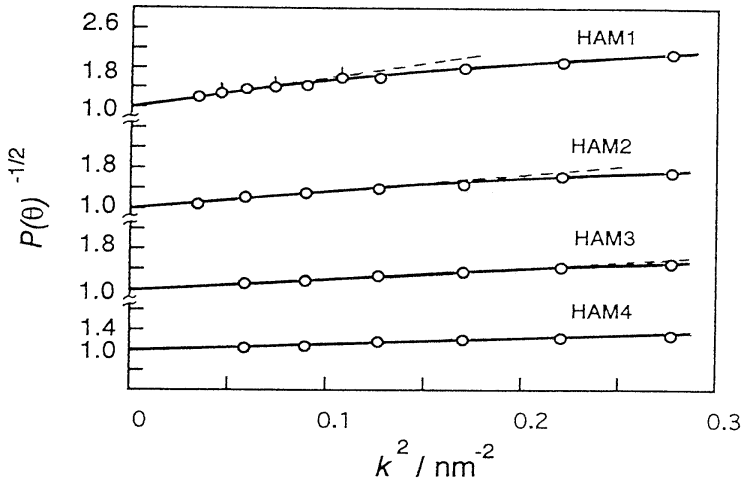| Sample	$10^{-3}M_w$	M_z/M_w	$<S^2>_z^{1/2}$ / nm		$[\eta]$ / cm^3 g^{-1}	
			$C_s = 0.02$ M	0.1 M	0.02 M	0.1 M
HAM1	11.0	1.1$_8$	5.9	5.5	38.6	33.2
HAM2	7.69	1.1$_4$	4.5	4.2	25.6	22.0
HAM3	5.92	1.1$_1$	3.6	3.4	20.2	17.6
HAM4	3.82	1.0$_4$	2.5	2.3	12.1	10.8

Figure 1. Angular dependence of $P(\theta)^{-1/2}$ for Na hyaluronate samples in 0.02 M aqueous NaCl at 25°C.

Table II. Wormlike Chain Parameters and Excluded-Volume Strength for Na Hyaluronate in Aqueous NaCl at 25°C[a]

C_s / M	M_L / nm^{-1}	q / nm	B / nm
0.02	405	6.0	9.0
0.1	410	4.8	4.8

a Taken from refs. 2 and 7.

Discussion

Radius of Gyration
In the QTP scheme (6), $<S^2>$ may be expressed by

$$<S^2> \ = <S^2>_0 \ [1 + 10\tilde{z} + (\frac{70\pi}{9} + \frac{10}{3})\tilde{z}^2 + 8\pi^{3/2}\tilde{z}^3]^{2/15}$$

$$\text{x } [0.933 + 0.067 \exp(-0.85\tilde{z} - 1.39\tilde{z}^2)] \tag{1}$$

if the Domb-Barrett function (10) is adopted for the radius expansion factor. Here, $<S^2>_0$ (the unperturbed mean-square radius of gyration) is given for the wormlike chain by (11)

$$\langle S^2\rangle_0 = (qL/3) - q^2 + (2q^3/L) - (2q^4/L^2)[1 - \exp(-L/q)] \qquad (2)$$

and $\tilde{z}$ is the scaled excluded-volume parameter defined by (12)

$$\tilde{z} = (3/4)Kz \qquad (3)$$

In these equations, L is the contour length of the chain, K is a known function of $L/2q$ (13), and z is the conventional excluded-volume parameter defined (with the present notation) by $z = (3/2\pi)^{3/2}(B/2q) \times (L/2q)^{1/2}$.

In Figure 2, the theoretical curves calculated from the above equations with the parameters in Table II are compared with the present $\langle S^2\rangle_z$ data and the previous light scattering data (7) at $C_s = 0.02$ and 0.1 M; the solid and dashed lines refer to the perturbed and unperturbed states, respectively. In both graphs, the agreement is fairly satisfactory. In particular, the fit of the line, solid or dashed, to the filled circles substantiates that for M_w below 1.1 x 10^4 the hyaluronate molecule at either salt concentration behaves like an unperturbed wormlike chain with the parameters in Table II; the slight upward deviations of these circles may be due to the polydispersity of our samples, though they are hardly beyond
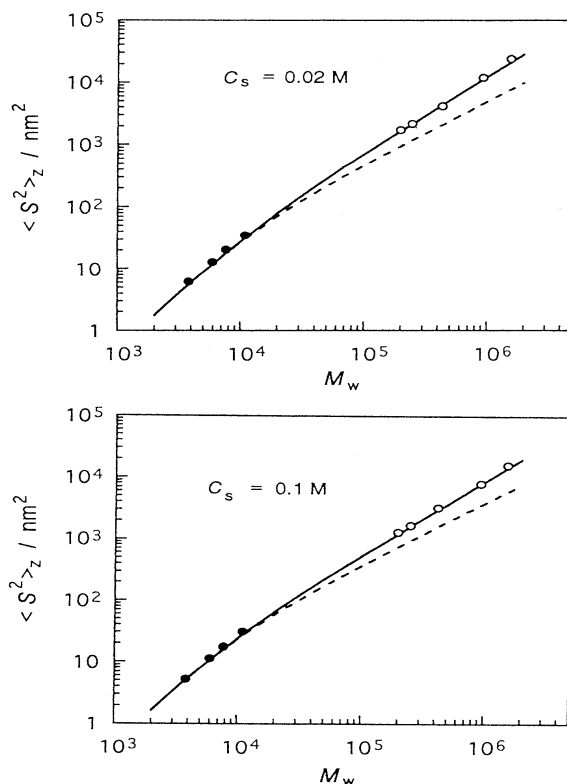

Figure 2. Comparison between the measured $\langle S^2\rangle_z$ (circles) and the theoretical values (solid lines) calculated from eq 1 with the parameters in Table II for Na hyaluronate in aqueous NaCl with $C_s = 0.02$ and 0.1 M. (●), from SAXS (this work); (○), from light scattering (7). The dashed lines represent the theoretical values (eq 2) in the unperturbed state.

the experimental uncertainty.

Scattering Function

The measured $P(\theta)$ generally contains the contribution from the chain thickness, whereas the theoretical function $P_0(\theta)$ available for unperturbed wormlike chains (14) is associated with the chain contour. Such a difference arising from the chain thickness is 2.5% even for $k = 0.9$ nm^{-1} when estimated by the conventional relation $P(\theta) = P_0(\theta) \exp[-(kd)^2/16]$ for a straight cylinder (15,16), with the diameter d taken as 0.7 nm (the value calculated from the partial specific volume). On the basis of this estimate, we ignore the difference between $P(\theta)$ and $P_0(\theta)$ in the present analysis.

The theoretical curves (the solid lines) for the unperturbed wormlike chains (14) with the q and M_L values in Table II are compared with the experimental scattering functions (the circles) in the form of the Kratky plot for sample HAM1 ($L = 27.2$ nm) at $C_s = 0.02$ M in Figure 3 and for sample HAM3 ($L = 14.4$ nm) at $C_s = 0.1$ M in Figure 4. They come close to the data points in the respective figures, leading to the conclusion that the q and M_L values estimated from $[\eta]$ are consistent not only with the present $\langle S^2 \rangle_z$ data but also with the $P(\theta)$ data.
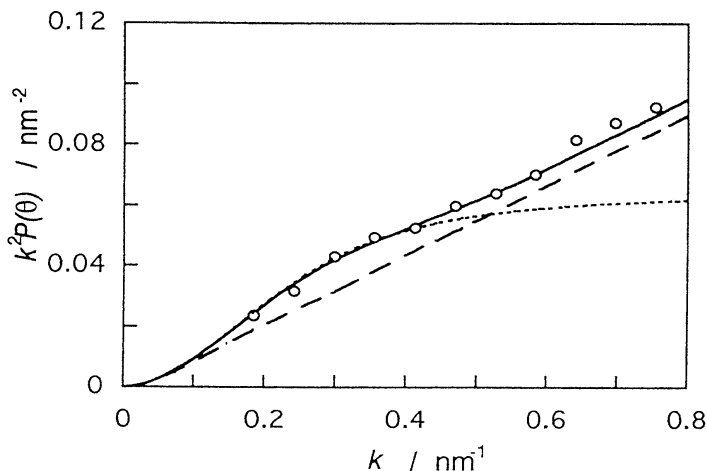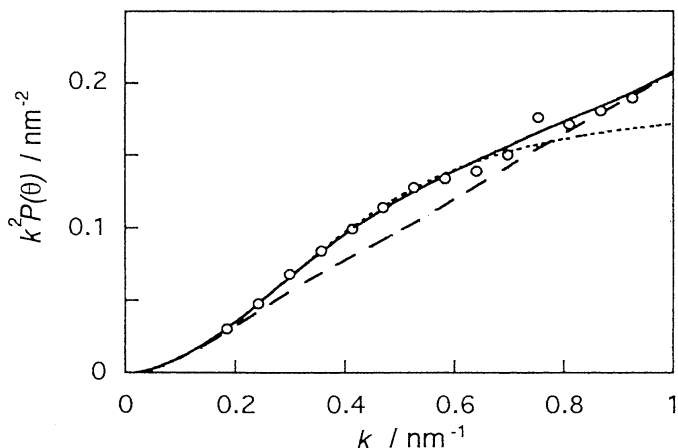

Figure 3. Comparison between the theoretical and experimental scattering functions in the form of the Kratky plot. (O), sample HAM1 in 0.02 M aqueous NaCl; (———), theoretical values (14) for the unperturbed wormlike chain with $q = 6.0$ nm and $M_L = 405$ nm^{-1}. See the text as for the dotted and dashed lines.

Figure 4. Comparison between the theoretical and experimental scattering functions in the form of the Kratky plot. (O), sample HAM3 in 0.1 M aqueous NaCl; (——), theoretical values (14) for the unperturbed wormlike chain with q = 4.8 nm and M_L = 410 nm^{-1}. See the text as for the dotted and dashed lines.

The dotted curve in either figure represents the Debye function (17) for the Gaussian chain with the same $<S^2>$ as that of the wormlike chain under consideration and the dashed one, the scattering function (17) for the thin rod with the same L as that of the wormlike chain. It can be seen in Figure 3 that as k increases, the experimental scattering function continuously changes from the Gaussian to rodlike behavior. This is a typical feature of the unperturbed wormlike chain. Similar behavior was also found for the same sample (HAM1) at C_s = 0.1 M. As M_w lowered, the approach to the asymptotic rod behavior at both 0.02 and 0.1 M became less definitive in the k range examined. Figure 4 exemplifies this.

In conclusion, the present data of $<S^2>_z$, $P(\theta)$, and $[\eta]$ for Na hyaluronate samples with $M_w \leq 1.1$ x 10^4 in 0.02 and 0.1 M aqueous NaCl are all consistently explained by the unperturbed wormlike chain. Thus, our recent analysis (7) of light scattering data mentioned in the Introduction can now be taken to show that the QTP theory for nonionic chains is applicable, in a good approximation, to both $<S^2>$ and $[\eta]$ of the charged polysaccharide in aqueous NaCl unless C_s is lower than 0.02 M.

References
 1. Hayashi K, Tsutsumi K, Nakajima F, Norisuye T, Teramoto A (1995) Macromolecules 28: 3824
 2. Hayashi K, Tsutsumi K, Norisuye T, Teramoto A (1996) Polym J 28: 922
 3. Yamakawa H, Fujii M (1974) Macromolecules 7: 128
 4. Yamakawa H, Yoshizaki T (1980) Macromolecules 13: 633
 5. Kratky O, Porod G (1949) Rec Trav Chim (Pays Bas) 68: 1106
 6. Yamakawa H (1997) Helical Wormlike Chains in Polymer Solutions. Springer, Berlin
 7. Tsutsumi K, Norisuye T Submitted to Polym J
 8. Nakamura Y, Akashi K, Norisuye T, Teramoto A, Sato M (1997) Polym Bull 38: 469
 9. Akashi K, Nakamura Y, Norisuye T Polymer (in press)
10. Domb C, Barrett AJ (1976) Polymer 17: 179
11. Benoit H, Doty P (1953) J Phys Chem 57: 958
12. Yamakawa H, Stockmayer WH (1972) J Chem Phys 57: 2843
13. Shimada J, Yamakawa H (1986) J Chem Phys 85: 591
14. Yoshizaki T, Yamakawa H (1980) Macromolecule 13: 1518
15. Porod G (1982) In: Glatter O, Kratky O (eds) Small Angle X-Ray Scattering. Academic Press New York pp 17
16. Nagasaka K, Yoshizaki T, Shimada J, Yamakawa H (1991) Macromolecules 24: 924
17. See, for example, ref. 14